JOURNAL OF MATERIALS SCIENCE: MATERIALS IN MEDICINE **16** (2005) 319–324

Precipitation of hydroxyapatite nanoparticles: Effects of precipitation method on electrophoretic deposition

M. WEI*
Department of Metallurgy and Materials Engineering, University of Connecticut, CT 06269, USA
E-mail: m.wei@ims.uconn.edu

A. J. RUYS
Department of Biomedical Engineering, School of Aerospace Mechanical and Mechatronic Engineering, University of Sydney, NSW 2006, Australia

B. K. MILTHORPE
Graduate School for Biomedical Engineering, University of New South Wales, NSW 2052, Australia

C. C. SORRELL
School of Materials Science and Engineering, University of New South Wales, Sydney, NSW 2052, Australia

Electrophoretic deposition is a low-cost, simple, and flexible coating method for producing hydroxyapatite (HA) coatings on metal implants with a broad range of thicknesses, from <1 μm to >500 μm. As for many other HA coating techniques, densification of electrophoretically deposited coatings involves heating the coated metal to temperatures above 1000 °C. Metal substrates tend to react with HA coatings at such temperatures inducing decomposition at temperatures below 1050 °C (decomposition for pure HA normally occurs above 1300 °C). Therefore, densification of these coatings needs to be conducted at temperatures lower than 1050 °C, and this necessitates the use of high-surface-area HA nano-precipitates, rather than commercially available pre-calcined powders, which densify at temperatures typically higher than 1200 °C. HA nano-precipitates were prepared by three methods and deposited on metal substrates by electrophoresis: (1) the *acid base* method, which produced plate-like nano-particles with a 2.5:1 aspect ratio, and severely cracked coatings; (2) the *calcium acetate* method, which produced needle-like nano-particles with a 10:1 aspect ratio, and slightly cracked coatings; (3) the *metathesis* method, which produced rounded nano-particles with a 2:1 aspect ratio, and high-quality crack-free coatings. The results suggested that the less equiaxed the nano-particles, the more cracked the coatings obtained by the electrophoretic deposition technique.

1. Introduction

Hydroxyapatite (HA) [$Ca_{10}(PO_4)_6(OH)_2$] is the main mineral component of bone and its synthetic form is one of the few materials capable of forming a direct chemical bond with bone *in vivo* [1]. However, the mechanical properties of HA are poor, rendering it unsuitable for load-bearing applications [2]. One solution to this problem is metal-fiber reinforcement. A recent study has demonstrated that the toughness of HA can be enhanced up to fourteen times via metal fiber reinforcement, giving it a toughness similar to cortical bone [3]. The other solution to this problem is the deposition of HA coatings on metal implants, thereby combining the toughness and load bearing capabilities of the metal with the bioactivity of the HA. Deposition of HA coatings has been achieved by a number of methods including [4–9]:

1. Plasma spraying [4]
2. Pulse laser deposition [5]
3. Electrochemical deposition [6]
4. Sol-gel coating [7]
5. Biomimetic coating [8]
6. Electrophoretic deposition [9]

*Author to whom all correspondence should be addressed.

Electrophoretic deposition (EPD) is a flexible, rapid, low cost process capable of rapid deposition rates (seconds to minutes) with a high degree of control over deposition thickness and morphology, and the ability to produce coatings on metal implants with a broad range of thicknesses from $<1\ \mu$m to $>500\ \mu$m. Electrophoresis involves the migration of charged colloidal-sized particles (not ions) towards the counter-charged electrode at which deposition occurs. Positively charged particles deposit on the cathode (cataphoresis), and negatively charged particles deposit on the anode (anophoresis) [10]. Currently, significant research attention has been focused on the thermal spray process for depositing HA coatings on metals. The main advantages of EPD over thermal spraying are the low processing cost and the fact that EPD is a non line-of-sight process and so can be used to evenly coat substrates of complex shapes or morphologies. The main disadvantage is that EPD coatings must be densified after deposition, and this involves heating the coated metal implant to temperatures in excess of 800 °C. Heating is problematic in terms of degradation of the HA coating and deterioration of the metal substrates.

Temperatures above 900 °C can potentially have deleterious effects on titanium and stainless steel implants, principally via surface oxidation and phase changes that spoil the mechanical properties. Therefore, densification needs to be conducted at as low a temperature as possible and in a highly oxygen-depleted furnace atmosphere. A recent study by the authors has demonstrated that an oxidation layer was formed on the surface of HA coated metallic substrates at an elevated temperature, which became an potential weak layer for the bonding between HA and the metal [11].

Elevated temperatures can also be deleterious for the HA coating. Previous studies have demonstrated that additions of fibres or particles to an HA matrix reduces its decomposition temperature from the usual range of ∼1300–1400 °C (pure HA) down to ∼750–1150 °C [12–14]. Decomposition is undesirable since it results in an enhanced *in vitro* dissolution rate for the HA [15]. The degree of reduction in decomposition temperature depends on the chemical composition of the additive, and the amount of additives in HA. In the case of 316L stainless steel particles, the decomposition temperature was reduced to ∼950 °C [14], and in the case of titanium particles, the decomposition temperature was reduced to ∼1050 °C [13]. In both cases, the addition was 10 to 20 vol% of metal particles to the HA with a metal particle size of tens of microns, i.e., the metal particle diameter is comparable to the thickness of a typical HA coating on a metal substrate, so the reaction zone was of comparable dimensions. Since the interfacial interaction in a thin-HA-coating/metal-substrate scenario would be similar to the interfacial interaction in particle or fiber reinforced HA, these decomposition temperatures would be good guides for determining the sintering temperature in the current study.

Therefore, relatively low sintering temperature is desirable for the HA coated metal system. Minimization of the HA densification temperature requires the use of HA powders with maximal specific surface area. Densification of HA follows a sigmoidal correlation with a characteristic plateau temperature and plateau density, which is typically in the order of 1150–1300 °C and 80–95% dense for commercial pre-calcined powders [16, 17]. Only with as-precipitated uncalcined powders can approach the 100% density plateau at a temperature as low as 950–1000 °C [16, 18]. Therefore, the present study investigated the effects of as-precipitated HA powders, rather than commercially available calcined powders.

TABLE I Reported processes for the precipitation of $Ca_{10}(PO_4)_6(OH)_2$ (HA) [11]

A. Dry Processes

1. $3Ca_3(PO_4)_2 + CaO + H_2O \rightarrow Ca_{10}(PO_4)_6(OH)_2$
2. $3Ca_2P_2O_7 + 4CaCO_3 + H_2O \rightarrow Ca_{10}(PO_4)_6(OH)_2 + 4CO_2$
3. $CaHPO_4 + 4CaCO_3 \rightarrow Ca_{10}(PO_4)_6(OH)_2 + 2H_2O + 4CO_2$

B. Wet processes

1. $12CaCl_2 + 8H_3PO_4 + 2H_2O \rightarrow Ca_{10}(PO_4)_6(OH)_2 + 2CaHPO_4 + 24HCl$
2. $10Ca(NO_3)_2 + 6KH_2PO_4 + 2H_2O \rightarrow Ca_{10}(PO_4)_6(OH)_2 + 6KNO_3 + 14\ HNO_3$
3. $10Ca(OH)_2 + 6H_3PO_4 \rightarrow Ca_{10}(PO_4)_6(OH)_2 + 18H_2O$
4. $10Ca(NO_3)_2 + 6(NH_4)_2HPO_4 + 2H_2O \rightarrow Ca_{10}(PO_4)_6(OH)_2 + 12NH_4NO_3 + 8HNO_3$
5. $10Ca(NO_3)_2 + 6NH_4H_2PO_4 + 8NH_4OH \rightarrow Ca_{10}(PO_4)_6(OH)_2 + 20NH_4NO_3 + 6H_2O$
6. $10Ca(CH_3COO)_3 + 6(NH_4)_2HPO_4 + 8NH_3 + H_2O \rightarrow Ca_{10}\ (PO_4)_6(OH)_2 + 20CH_3COONH_4$

C. Hydrothermal processes

1. $10CaHPO_42H_2O \rightarrow Ca_{10}(PO_4)_6(OH)_2 + 4H_3PO_4$
2. $10CaHPO_4 + 2H_2O \rightarrow Ca_{10}(PO_4)_6(OH)_2 + 4H_3PO_4$

A number of methods can be used to precipitate HA, and these are compiled in Table I. In this study, the focus was on three wet chemical methods:

The *acid base* method (method B3 in Table I): This involves a neutralisation reaction between lime and phosphoric acid at a pH higher than 9.5 [19, 20]. This is probably the most commonly used method for synthesis of HA powders commercially since it is a simple process that uses low-cost raw materials.

The *calcium acetate* method (method B6 in Table I): This is essentially an acid-catalysed alkoxide reaction [14]. Being an alkoxide process, it does not compete favourably with the *acid base* method in economic terms and so it is not commonly used commercially.

The *metathesis* method (method B5 in Table I): This involves the precipitation of calcium phosphate and subsequent alkali digestion in aqueous ammonia at a pH of 11–12 [22, 23]. Although it is somewhat more complex and costly than the *acid base* method, it can yield superior quality HA powders. Therefore it is quite commonly used in HA research, though less commonly used commercially.

2. Materials and methods

HA powders were prepared using each of the three methods: *acid base* [20], *calcium acetate* [21], and *metathesis* [22, 23].

Acid base synthesis:

1. 5.0 g of $Ca(OH)_2$ (∼99%, Sigma Chemical Co., USA) was dissolved in 200 ml of de-ionized water using a magnetic stirrer.

2. 4.669 g of liquid H_3PO_4 (85%, BDH Limited, Poole, England) was added slowly (at 1 to 2 ml/min so as to maintain pH > 9.5–10) to the $Ca(OH)_2$ solution while the solution was continuously stirred by the magnetic stirrer. The solution pH value was continuously monitored using a pH meter (Model R-103 pH/mV Meter, Activon Scientific Products Co. Pty. Ltd., Australia).

3. After the H_3PO_4 addition stage, the HA precipitate was washed by thrice repeating the following three steps: centrifugation, supernatant decantation, and re-suspension in de-ionized water.

Calcium acetate synthesis:

1. 10 g of $(NH_4)_2HPO_4$ (98%, Ajax Chemicals, Australia) was dissolved into 126 ml of de-ionized water. The pH of the solution was measured using a pH meter (∼8.0).

2. 20 g of $Ca(CH_3COO)_3$ (Dried, 98+%, Aldrich Chemical Company Inc., USA) was dissolved into 300 ml de-ionized water (pH ∼ 8.2). 15 ml of strong ammonia (28–30%, Ajax Chemicals, Australia) was added to adjust the pH value of the solution to 11, and then 190 ml de-ionized water was added.

3. The $(NH_4)_2HPO_4$ solution was slowly added dropwise into the $Ca(CH_3COO)_3$ solution at a rate of 10 ml/min through a filter funnel containing filter paper, while vigorously stirring with a magnetic stirrer.

4. The mixed solution was heated to 40 °C for 3 h by continuous stirring on a hot plate.

5. The solution was allowed to cool to room temperature and the precipitate was then separated from the water by repeating the following three steps: centrifugation, supernatant decantation, and re-suspension in de-ionized water.

Metathesis synthesis:

1. 47.22 g of $Ca(NO_3)_2{\cdot}4H_2O$ (99.0%, Ajax Chemicals, Australia) and 6 ml of strong ammonia solution were added to 180 ml de-ionized water and mixed using a magnetic stirrer.

2. The pH of this solution was adjusted to ∼12 with the strong ammonia, and then 174 ml de-ionized water was added to the above solution, named solution 1.

3. 15.84 g of $(NH_4)_2HPO_4$ (98%, Ajax Chemicals, Australia) and 150 ml of strong ammonia were mixed with 300 ml of de-ionized water.

4. The pH of this solution was adjusted to ∼12, and then 190 ml de-ionized water was added to this solution, thereby dissolving the precipitate and forming solution 2.

5. Solution 2 was slowly added to solution 1 at a rate of 80–100 ml/min, while vigorously stirring with a magnetic stirrer.

6. The resulting suspension was then placed on a magnetic stirrer/hot plate, heated to boiling point, then stirred at boiling point for 1 h.

7. The suspension was then cooled and aged at room temperature for 20 days.

8. The HA precipitate was then washed by thrice repeating the following three steps: centrifugation, supernatant decantation, and re-suspension in de-ionized water.

Dilute ethanol suspensions of the HA nano-precipitates were prepared by adding 1.5 g of HA powder to 100 ml of ethanol in a 200 ml glass beaker, and ultrasonically dispersing in a 50 kHz ultrasonic bath (SCAN DIA B-220, Germany) for 30 min. The apparatus for electrophoretic coating is illustrated in Fig. 1. The distance between the two electrodes was approximately 6 mm. The electrodes were placed parallel to each other in the suspension, and connected to a high-voltage power supply (Power Supply, BIO-RAD, Model 500/200, Australia). The deposition conditions were 200 V/20 s. The coated specimens were slowly dried in a sealed dessicator at room temperature. The coating thickness was approximately 30 μm for all the three HA precipitates.

The HA powders were positively charged in the solution, moving towards the cathode under the influence of the electric field and depositing there. The anode comprised a 10 × 50 mm copper strip and the cathode (deposition electrode) comprised a 5 × 45 × 3 mm Ti6Al4V alloy substrate. Before deposition, the Ti6Al4V substrate was sandblasted with commercial garnet (Sandblasting and Metallizing Service Pty. Ltd., Australia) and its surface roughness was measured using a fine probe at a number of locations and the arithmetic mean determined (Alpha-Step 200, Tencor Instruments, USA). Before deposition, the sandblasted substrates were thoroughly washed with a commercial detergent (Diversey, pyrogenically negative cleaner, Australia) in an ultrasonic bath for ∼30 min, followed by washing in acetone (95.9%, Ajax Chemicals, Australia) for another 15 min, then passivated in 25 vol% nitric acid (69.0–71.0%, Ajax Chemicals, Australia) overnight.

The phase composition of each powder was assessed by x-ray diffraction (Siemens D5000). The size and morphology of the precipitated HA nano-particles were assessed by field-emission scanning electron microscopy (FESEM: Hitachi S-900). FESEM specimens were prepared by deposition of an alcohol suspension of

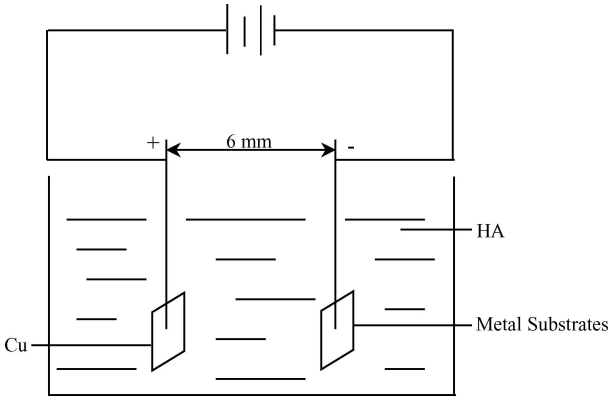

Figure 1 The electrophoretic deposition apparatus.

the HA nano-precipitate onto a brass stub, followed by drying, then coating with a 3 nm film of chromium (Dynavac, Xenosput 2000). The electrophoretically coated Ti6Al4V specimens were attached to 25 mm diameter aluminum sample holders using silver paste and then gold-coated (SEM Coating Unit E5000, Polaron Equipment Limited, USA) for scanning electron microscopy (SEM: Stereoscan S360, Cambridge Instruments, USA). In this way, the nano-particle morphology (by FESEM) could be correlated with coating characteristics (by SEM).

3. Results and discussion

The X-ray diffraction patterns of each of the three HA nano-precipitates are shown in Fig. 2. These X-ray charts reveal that HA powders produced by each of the three methods, *acid base*, *calcium acetate*, and *metathesis*, consisted of moderately crystalline hydroxyapatite. Pure hydroxyapatite was achieved by each method with no anhydrous calcium phosphate phases present.

FESEM micrographs of each powder are shown in Figs 3–5 revealing that the *acid base* method produced agglomerated plate-like nano-particles (~110 nm by ~45 nm, aspect ratio ~2.5:1), the *calcium acetate* method produced long sharp acicular nano-particles (~185 nm by ~20 nm, aspect ratio ~10:1), and the *metathesis* method produced fine, rounded, and elongated nano-particles (~90 nm by ~40 nm, aspect ratio ~2:1).

The effects of precipitation methods on coating characteristics are shown in the SEM micrographs of Figs 6–8 revealing that the *acid base* powder had the worst coating characteristics (severely cracked), the *calcium acetate* powder produced slightly cracked coatings, and the *metathesis* powder produced high-quality crack-free coatings. Obviously, the morphology of the HA particles had significant impact on the electrophoretic coating quality: the best coatings were obtained by the rounded particles, while acicular particles resulted in some cracking, and platy particles caused severe cracking.

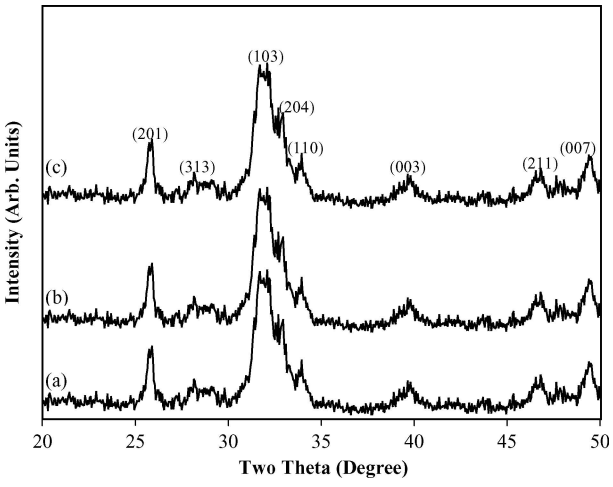

Figure 2 X-ray diffraction patterns for HA nanoparticles produced by each of the three methods: (a) *acid base*, (b) *calcium acetate*, and (c) *metathesis*.

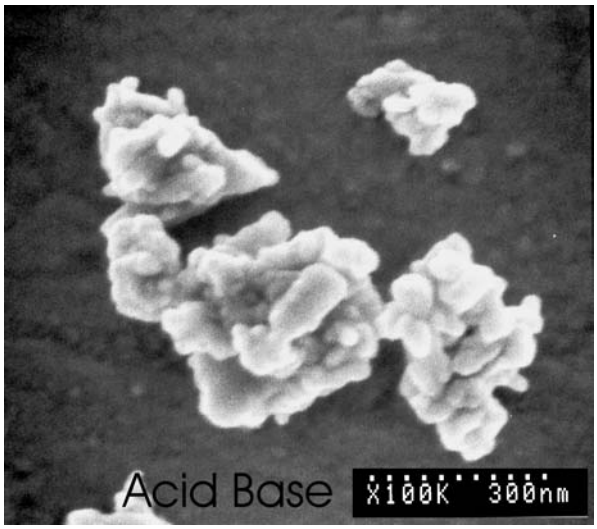

Figure 3 FESEM micrograph of HA nanoparticles produced by the *acid base* method.

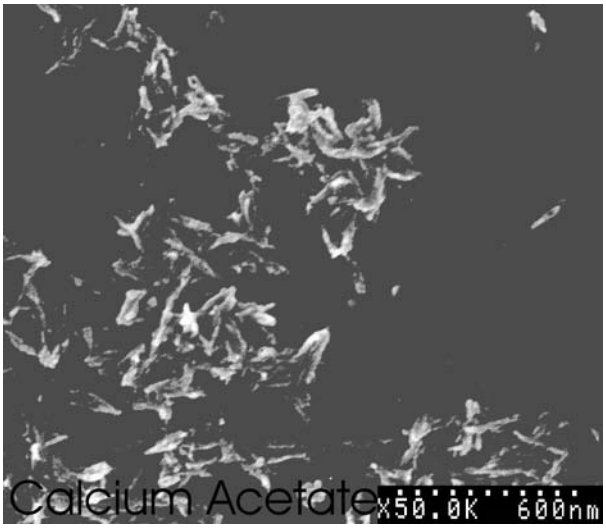

Figure 4 FESEM micrograph of HA nanoparticles produced by the *calcium acetate* method.

Figure 5 FESEM micrograph of HA nanoparticles produced by the *metathesis* method.

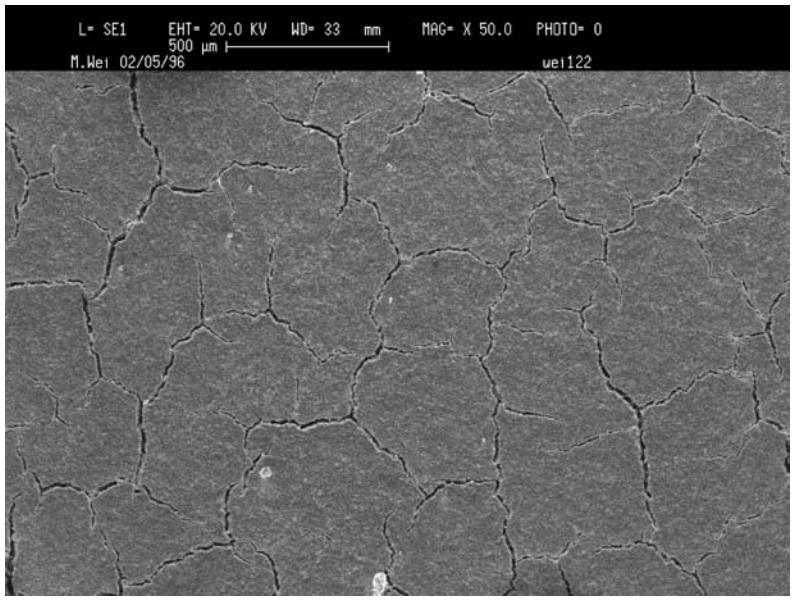

Figure 6 SEM micrograph of the electrophoretic coating produced with *acid base* HA.

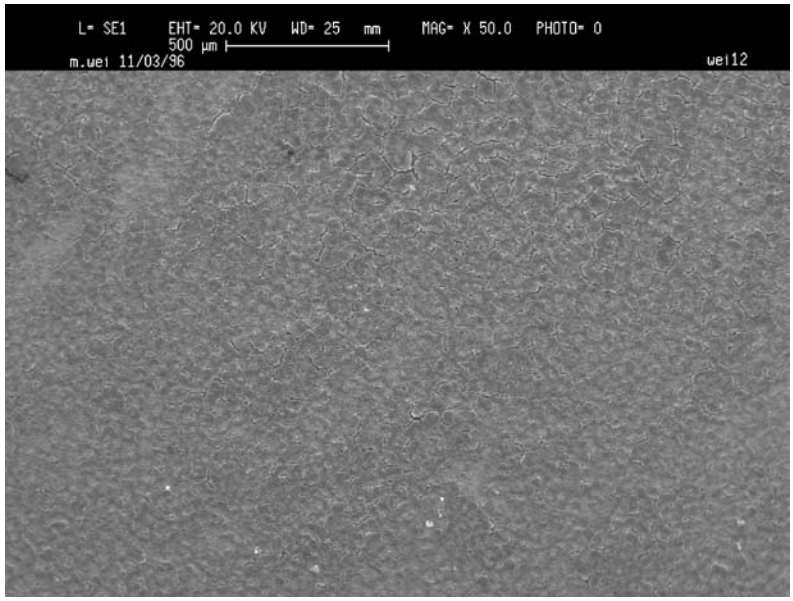

Figure 7 SEM micrograph of the electrophoretic coating produced with *calcium acetate* HA.

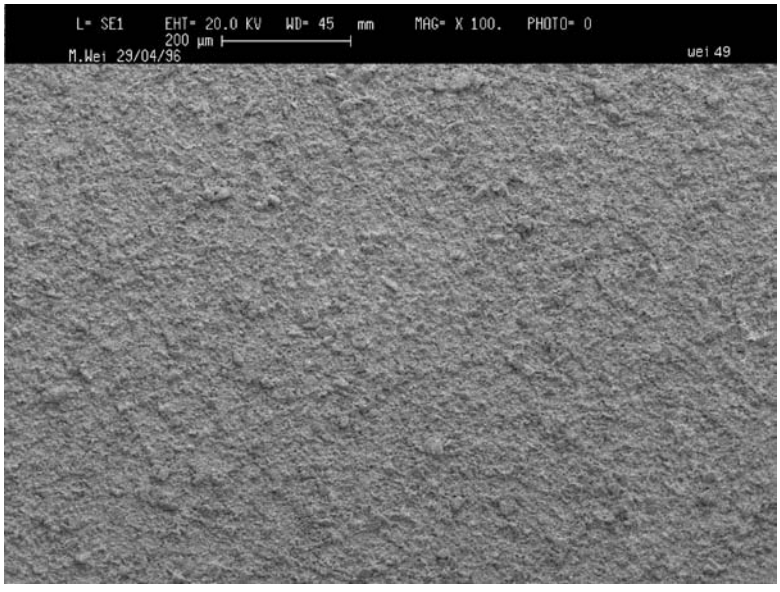

Figure 8 SEM micrograph of the electrophoretic coating produced with *metathesis* HA.

Cracking arises as a result of shrinkage during drying. Therefore, the smallest amount of drying shrinkage results in the lowest cracking susceptibility. For a given degree of shrinkage, the use of drying control chemical additives (DCCA's) can minimize the associated degree of cracking [24]. However, the ideal approach to minimizing cracking is to minimize drying shrinkage. Drying shrinkage is minimized by the use of regularly shaped particles that can pack efficiently, large particle size distributions for gap-graded efficient packing, and large particle sizes. Since all three nano-particle types investigated in this study were very fine and of fairly narrow size distributions, the only significant differentiating feature between them was particle shape.

The *metathesis* particles had the most regular shape: rounded with an aspect ratio of ~2:1, i.e., regular in two axes (width and depth), and almost regular in the third axis (length), with the result that cracking did not occur. The *calcium acetate* particles had the next most regular shape: they were regular in two axes (width and depth), and highly irregular in the third axis (length), with the result that only moderate amounts of cracking occurred. The *acid base* nano-particles had the most irregular shape of all: plates, irregular in all three axes, with the result that cracking was severe.

Therefore, cracking susceptibility appeared to be dependent on the shape of the HA nano-particles with the best results achieved with the most regular particle shape, as produced by the *metathesis* method. Therefore, it has been demonstrated that cracking can be eliminated with such fine (nano-particulate) particles provided that their shape is close to equi-axed.

4. Conclusions

1. The *acid base* method produced plate-like nano-particles of an approximately 2.5:1 aspect ratio and poor quality cracked coatings.

2. The *calcium acetate* method produced fine acicular nano-particles of an approximately 10:1 aspect ratio, and moderately poor coatings.

3. The *metathesis* method produced fine rounded nano-particles of an approximately 2:1 aspect ratio, and high-quality crack-free coatings.

4. The cracking susceptibility appeared to correlate with the particle shape: the more regular the particle shape (the closer it was to equi-axed), the less the cracking susceptibility.

Acknowledgments

The assistance of Dr C.H. Kong of the electron microscopy unit with the FESEM analysis is gratefully acknowledged.

References

1. J. B. PARK and R. S. LAKES, "Biomaterials: An Introduction" (Plenum Press, New York, 1992).
2. A. RAVAGLIOLI and A. KRAJEWSKI, "Bioceramics: Materials, Properties, Applications" (Chapman & Hall, London, 1992).
3. A. J. RUYS, N. EHSANI, B. K. MILTHORPE, K. HUSSLEIN, M. KOSCHIG and C. C. SORRELL, in Proceedings. Pacrim II: Second International Symposium of Pacific Rim Ceramic Societies, edited by P. A. Walls, C. C. Sorrell and A. J. Ruys (Australasian Ceramic Society, Cairns, 1997), p. 45.
4. K. A. GROSS, N. RAY and M. ROKKUM, *J. Biomed. Mater. Res.* **63** (2002) 106.
5. H. ZENG and W. R. LACEFIELD, *ibid.* **50** (2000) 239.
6. R. CHIESA, E. SANDRINI, M. SANTIN, G. RONDELLI and A. CIGADA, *J. Appl. Biomat. Biomech.* **1** (2003) 91.
7. A. MILEV, G. S. K. KANNANGARA and B. BENNISSAN, *Mater. Lett.* **57** (2003) 1960.
8. M. WEI, M. UCHIDA, H. KIM, T, KOKUBO and T. NAKAMURA, *Biomater.* **23** (2001) 167.
9. M. WEI, A. J. RUYS, B. K. MILTHORPE, C. C. SORRELL and J. H. EVANS, *J. Sol-Gel Sci. Tech.* **21** (2001) 39.
10. J. B. BIRKS and J. H. SCHULMAN, "Progress in Dielectrics. Volume I" (Heywood & Company Ltd., London, 1959).
11. M. WEI, A. J. RUYS, B. K. MILTHORPE and C. C. SORRELL, *Mater. Eng.* **9** (1998) 7.
12. A. J. RUYS, A. BRANDWOOD, B. K. MILTHORPE, M. R. DICKSON, K. A. ZEIGLER and C. C. SORRELL, *J. Mater. Sci. Mater. Med.* **6** (1995) 297.
13. A. J. RUYS, N. EHSANI, B. K. MILTHORPE and C. C. SORRELL, *J. Aust. Ceram. Soc.* **29** (1993) 65.
14. A. J. RUYS, K. A. ZEIGLER, B. K. MILTHORPE and C. C. SORRELL, in "Ceramics: Adding the Value," edited by M. J. Bannister (CSIRO, Melbourne, 1992) p. 591.
15. P. DUCHEYNE, S. RADIN, M. HEUGHEBAERT and J. C. HEUGHEBAERT, *Biomater.* **11** (1990) 244.
16. A. J. RUYS, C. C. SORRELL, A. BRANDWOOD and B. K. MILTHORPE, *J. Mater. Sci. Lett.* **14** (1995) 744.
17. A. J. RUYS, M. WEI, C. C. SORRELL, M. R. DICKSON, A. BRANDWOOD and B. K. MILTHORPE, *Biomater.* **16** (1995) 409.
18. W. LI and L. GAO, *Guocheng Gongcheng Xuebao* **2** (2002) 305.
19. H. TAGAI and H. AOKI, "Mechanical Properties of Biomaterials" (John Wiley, New York, 1980).
20. B. F. YETER-DAL, V. GROSS and T. W. TURNEY, in "Ceramics: Adding the Value," edited by M. J. Bannister (CSIRO, Melbourne, 1992) p. 617.
21. T. FUTAGAMI and T. OKAMOTO, *J. Ceram. Soc. Japan.* **95** (1987) 775.
22. M. JARCHO, C. H. BOLEN, M. B. THOMAS, J. BOBICK, J. F. KAY and R. H. DOREMUS, *J. Mater. Sci.* **11** (1976) 2027.
23. M. WEI, T. BOSTROM, L. GRØNDAHL and J. H. EVANS, *J. Mater. Sci. Mater. Med.* **14** (2003) 311.
24. K.-M. HUNG and W.-D. YANG, *Mater. Manuf. Proc.* **17** (2002) 323.

Received 2 March
and accepted 17 November 2004